Scientia Horticulturae 345 (2025) 114124

Contents lists available at ScienceDirect

Scientia Horticulturae

journal homepage: www.elsevier.com/locate/scihorti

Research Paper

Exploring dynamic nitrogen (N) fertigation guided by multispectral sensors: a sustainable optimization of N fertilization in processing tomato

Vito Aurelio Cerasola [a], Stefano Bona [b], Daniele Borsato [b], Luca Gavioli [a], Gaia Moretti [a], Luigi Manfrini [a], Giuseppina Pennisi [a,*], Francesco Orsini [a], Enrico Buscaroli [a], Paolo Sambo [b], Giorgio Gianquinto [a]

[a] Department of Agricultural and Food Sciences (DISTAL), Alma Mater Studiorum - University of Bologna, Viale Fanin 44, Bologna 40127, Italy
[b] Department of Agronomy, Food, Natural resources, Animals and Environment (DAFNAE), University of Padova, Viale dell'Università, 16, Legnaro, PD 35020, Italy

ARTICLE INFO

Keywords:
Precision agriculture
Nitrogen fertilization
Nitrogen use efficiency (NUE)
Dynamic N management
Vegetation index, Fertigation

ABSTRACT

Dynamic management of nitrogen (N) guided by multispectral sensors can help match in-season crop N requirements with precise N supply through fertigation. In the present work, different dynamic strategies to optimize N fertigation in processing tomatoes were explored in two plot experiments across two different years and locations, compared with a well-fertilized control (180 kg N ha^{-1}, N180). In dynamic N strategies, the green vegetation index (GVI) was monitored with a hand-held multispectral radiometer. Whenever the GVI fell below a critical threshold, N fertilizer was supplied via fertigation. Critical thresholds were developed using different approaches: in the spy plot strategy (N SPY), the N fertilizer was supplied whenever the GVI of the plot was below 90% of the GVI in the spy plot N180. Conversely, absolute threshold GVI values were developed in previous modeling stages based on linear-plateau relationships between the GVI and the relative yield (N THR strategies) or based on the monitoring of the GVI profile of tomatoes under non-limiting N conditions in a previous growing season (N SPY_{EVO}). In general, the dynamic N strategies saved a significant amount of N fertilizers (with reductions ranging from 38 to 60%), with best performances observed for the N THR and N SPY_{EVO}. Dynamic N strategies did not penalize the marketable yield, thus, the N use efficiency, the fertilizer costs, and the greenhouse gas emission intensity associated with the fertilization were significantly optimized. Furthermore, dynamic N strategies produced fewer but bigger fruits. The present work shows innovative N management strategies to optimize N inputs in processing tomato cultivation, confirming the potential of multispectral sensors in precision agriculture.

1. Introduction

Nitrogen (N) stands out as an essential nutrient for crops, as it is a fundamental constituent of proteins, chlorophyll, and nucleic acids, all crucial for vital metabolic processes. Consequently, N fertilizers play a key role in enhancing crop productivity, contributing to ensuring food security and reducing malnutrition (Peñuelas et al. 2023). Notwithstanding, vegetable farmers often view N fertilizers as a simple tool to boost productivity and mitigate economic losses, often leading to excessive applications (Tei et al. 2020). Coupled with the frequent over-irrigation and the shallow root apparatus of vegetable crops, this practice increases the risk of nitrate (NO_3^-) leaching, contributing to the eutrophication of water bodies. Moreover, excessive N fertilizer supplies lead to NO_3^- denitrification in soil, resulting in increased emissions of nitrous oxide (N_2O), a potent greenhouse gas (GHG) with a global warming potential 265 times greater than CO_2 (Menegat et al. 2022). According to Menegat et al. (2022), N fertilizers supply chains accounts for approximately 10.6% of total agricultural GHG emissions, and 2.1% of global GHG emissions. Therefore, it is clear that N fertilizer management is central in the dichotomy between food security and environmental protection (Peñuelas et al. 2023). The global inefficiencies in N fertilizer management reduce nitrogen use efficiency (NUE) in cropping systems: indeed, globally only about 55% of the N fertilizers applied are absorbed by crops, although such value is heavily influenced by the local socioeconomic context (Valenzuela 2024). Additionally, the price of N fertilizers is significantly influenced by the geopolitical

* Corresponding author.
E-mail address: giuseppina.pennisi@unibo.it (G. Pennisi).

https://doi.org/10.1016/j.scienta.2025.114124
Received 25 September 2024; Received in revised form 3 April 2025; Accepted 7 April 2025
Available online 15 April 2025

scenario (e.g., the Ukraine-Russia conflict), which adversely impacts farm profitability and ultimately results in higher food prices (Zeka and Skreli 2022; Hebebrand and Laborde 2023). Therefore, optimizing NUE is a crucial priority to alleviate environmental burdens and enhance the resilience of farming systems.

In vegetable cropping systems, N fertilizers are often supplied during crop growth through irrigation water (fertigation) (Gianquinto et al. 2011a). Here, the N fertilization is usually scheduled based on the farmer's experience or look-up-table adapted for different pedoclimatic conditions (Tei et al. 2020). However, to optimize NUE, the N fertilizer should be supplied when it is crucial for plant growth, matching the crop requirements at each growth stage. Such a method to manage the N fertilization, introduced as "dynamic optimization of N supply" already in the early nineties (Vos and Struik 1992), requires for the rapid assessment of the crop N status. Nowadays, optical sensors are among the quickest tools to assess crop N status. These include transmittance hand-held chlorophyll meters (Blackmer and Schepers 1995) and reflectance sensors. Reflectance sensors can involve proximal sensing, such as hand-held multispectral radiometers, or remote sensing tools, including unmanned aerial vehicles or satellites (Padilla et al. 2020). Multispectral radiometers are rapid tools capable of monitoring the crop reflectance at different wavelengths, which in turn is used to calculate vegetation indices related to crop N status (Gianquinto et al. 2011a). For instance, the Normalized Difference Vegetation Index (NDVI) and Red Vegetation Index (RVI) were the most sensitive indices for greenhouse indeterminate tomatoes (Padilla et al. 2015), and cucumber (Padilla et al. 2017), while the Green Vegetation Index (GVI) and Green Normalized Difference Vegetation Index (GNDVI) were the most reliable indices to assess the N status in open-field processing tomatoes (Gianquinto et al. 2011a). However, using such tools in scheduling N fertigation depends on the availability of threshold or reference values, below which the crops are considered in N starvation (Gianquinto et al. 2011b). Different methodologies have been developed to obtain such critical thresholds, and the spy plot strategy, also known as the reference plot strategy, is by far the most well-known in the scientific community. This strategy involves maintaining a plot with non-limiting N levels (spy plot) within the field: when the instrument's reading monitored in the field is below 90–95% of the reading from the spy plot, then N fertilizer should be supplied (Samborski et al. 2009). The spy plot strategy is the most diffused method to guide the N fertilization, but most studies focused on cereal crops (Samborski et al. 2009; Padilla et al. 2020). In cereal crops, precision N management strategy mainly relies on assessing the N status at the most sensitive growth stages, where the N fertilizers can be broadcast in the field. Conversely, in vegetable cropping systems, fertigation allows the farmer to potentially supply the N fertilizer whenever needed, as it does not involve any machinery entering the field and supplying the fertilizer as in the broadcast application. This implies that the precision N management techniques differ between cereal and vegetable crops since different fertilization methods are adopted, requiring a more frequent N status monitoring for the latter cropping systems. Although fewer studies are focused on vegetable crops (Padilla et al. 2020), the spy plot strategy proved to be efficient in cantaloupe cultivation, ensuring a drastic reduction of N supply down to 17–66% without yield reduction in comparison to control fertilization (Gianquinto et al. 2010), by 38–63% in potato (Fernandes et al. 2021), and by 25–44% in staked tomato (Oliveira et al. 2019). Despite the effectiveness of the spy plot strategy in enhancing NUE, its adoption by farmers is hindered by the need to split the field into two independent fertigation sectors. A promising alternative consists of adopting absolute threshold values of a N status index along the entire growing season. Two main methodological approaches exist to derive absolute threshold values: the first one, proposed by Gianquinto et al. (2004), relates the instrument reading (SPAD, or vegetation index) at different growth stages with the relative yield in linear-plateau models (Zheng et al. 2015; Padilla et al. 2017). The second approach consists of relating the instrument reading with the Nitrogen Nutrition Index (NNI), and the threshold is obtained by solving the equation for NNI=1 (Padilla et al. 2015; Rodríguez et al. 2020; Vadillo et al. 2022). Besides the approach adopted for building threshold curves, and the number of thresholds already developed, to the best of our knowledge, only Gianquinto et al. (2001) have tested the dynamic fertilization guided by absolute SPAD threshold values in potatoes, achieving up to 37–58% savings of N fertilizers compared to control fertilization, while maintaining the same yield level. Not only is this a matter of saving N fertilizers, but dynamic fertilization could also enhance the quality of the produce (Gianquinto et al. 2010) and be more profitable than conventional fertilization (Moreno-Garcìa et al. 2018).

Processing tomato (*Solanum lycopersicum* L.) stands among the most important vegetable crops in the world, and its productivity strongly depends on proper N fertilization (Petropoulos et al. 2020). Although threshold values of processing tomato exist for some tools (Gianquinto et al. 2004; Vadillo et al. 2022), their effectiveness for guiding N fertilization and improving the NUE was never explored. This paper tests different dynamic N management strategies at experimental plot level across two growing seasons and locations in Northern Italy using passive multispectral radiometers.

2. Materials and methods

2.1. Locations and experiments

Two experiments were carried out in two locations in Northern Italy. Experiment 1 (Exp. 1) was conducted at the experimental farm of the University of Padova in Legnaro (PD, 45°20′43 N 11°57′30″E, 8 m a.s.l.) in 2004, while Experiment 2 (Exp. 2) was carried out in 2023 at the experimental farm of the University of Bologna located in Cadriano (BO, 44°55′48″N, 11°41′31″E, 32 m a.s.l.). In the two experiments, the soil was prepared through tillage at 0.3 m and then harrowed before transplanting. Pests and weeds were controlled through the practices of the local farmers. Cultivars adopted in the experiments (Perfectpeel, and K2206) were developed by Seminis (St. Louis, Missouri, US) and ISI Sementi (Fidenza, Parma, Italy), respectively. The specific features of the experiments are reported in Table 1, and the applied treatments are detailed below.

In both experiments, traditional fertilization strategies were compared with the dynamic management of N guided by a multispectral radiometer. The Green Vegetation Index (GVI) was previously identified as the best-performing index for assessing the N status in processing tomatoes (Gianquinto et al. 2011a), and it was therefore used to guide N fertilization.

2.1.1. Experiment 1

In Exp. 1, tomato plants were transplanted on May 11, 2004, in a single-row system in isolated boxes (2 × 2 × 2 m) buried in the soil and filled with silty loam soil. The experiment included five N management strategies, replicated four times (for a total of 20 isolated boxes) in a complete randomized design. Plants were spaced 1 m between the rows and 0.3 m within the line, for a final planting density of about 30,000 plant ha^{-1}. Phosphorus was applied at the rate of 150 kg P_2O_5 ha^{-1} with superphosphate ($Ca_2(H_2PO_4)_2$, P_2O_5=46%), while 100 kg K_2O ha^{-1} was applied to fulfill the potassium requirements with potassium sulfate (K_2SO_4, K_2O=50%). Soil chemical-physical characteristics were as follows: pH (H_2O)=7.65, EC (Electrical Conductivity)=0.25 mS cm^{-1}, organic matter=1.45%, total *N*=0.95 g kg^{-1}, assimilable *P*=36 mg kg^{-1}, exchangeable *K*=102 mg kg^{-1}. Harvest occurred on August 26, 2004. The applied treatments were:

- Non-fertilized control (N0).
- Fertilized control (N180), where solid urea ($CO(NH_2)_2$, *N*=46%) was manually supplied at the rate of 180 kg N ha^{-1} to maintain the crop in non-limiting N conditions, following the typical N rate supply of local farmers. The N fertilizer application was split into three

Table 1
Details of the experiments carried out in Legnaro (PD) and Cadriano (BO). SL and SCL stand respectively for silty loam and silty clay loam.

Experiment	Season	Location	Cropping system	Soil	Treatment	Replicates	Cultivar	Multispectral radiometer
1	2004	Legnaro	Single row	SL	5	4	Perfectpeel	CropScan
2	2023	Cadriano	Single row	SCL	5	4	K2206	Spectrosense 2+

moments of the growing season (60 kg N ha^{-1} before the transplanting and, twice at soil coverage by the crop at 60 kg N ha^{-1} each). N180 was used as a spy plot to derive the GVI threshold in the N SPY strategy.
- N SPY, where the N fertilizer (calcium nitrate $Ca(NO_3)_2$, *N*=15.5%) was supplied through fertigation each time the sufficiency index (SI) was below 0.9 (Samborski et al. 2009). The sufficiency index was calculated as reported in Eq. (1):

$$Sufficiency\ index\ (SI) = \frac{GVI_{N\ SPY}}{GVI_{N180}} \quad (1)$$

- N THR, where critical GVI threshold curves were developed along the growing degree days (GDDs) and adopted for guiding the N fertilization. The critical GVI curve was developed from previous plot scale experiments using a linear-plateau relationship with the relative yield (Gianquinto et al. 2004), which is further detailed in the specific section. Whenever the GVI was below the critical GVI curve reduced by 10%, N fertilizer was supplied.
- N $THR_{15\%}$. This strategy reduced the critical GVI threshold curve developed from the fitting procedure by 15%. Then, similarly to N THR, the N fertilizer was applied whenever the GVI was below the critical GVI curve (yet reduced by 15%) and further reduced by 10%.

Notably, in the N SPY strategy, it is recommended to supply N whenever the SI is below 0.9, according to previous studies (Samborski et al. 2009; Ziadi et al. 2009; Cilia et al. 2014). To maintain consistency between the different dynamic strategies and make them comparable, the fitted curve of N THR and N $THR_{15\%}$ was reduced by 10% to trigger the fertigation. To check whether the reduced values of the critical threshold correspond to a yield reduction or not, in N $THR_{15\%}$, the fitted curve is reduced first by 15% and then again by 10% to trigger the fertigation.

A starter dose of N was supplied before the transplant at 30 kg N ha^{-1} for dynamic N strategies. Then, a small amount of N (between 10 and 25 kg N ha^{-1}) was supplied when recommended by the spectral reading to restore the optimal GVI. The N rate was adapted according to the crop phenological stage, and lower N rates (10 kg N ha^{-1}) were supplied until 50 days after transplant (DAT). Then, higher N rates were supplied until 65 DAT, when the highest LAI was reached (Tei et al. 2002), up to 25 kg N ha^{-1}. Then a gradual reduction back to 10 kg N ha^{-1} was performed during fruit ripening, when leaf senescence started occurring (Tei et al. 2002).

2.1.2. Experiment 2

In Exp. 2, tomato plants were transplanted on May 24, 2023, in experimental plots measuring 5 × 4 m. Five N strategies were compared, and each strategy was replicated four times in a complete randomized design in the experimental field, for a total of 20 independent experimental plots. A single-row system was adopted (1 m between the rows and 0.36 m within the row), resulting in 27,777 plants ha^{-1}. Superphosphate was broadcast in the soil at 90 kg P_2O_5 ha^{-1}, while potassium sulfate was supplied at the rate of 150 kg K_2O ha^{-1} via fertigation divided into three applications throughout the growing season. In this experiment, the soil was sampled at 0.3 m to determine chemical and physical characteristics. Soil chemical-physical characteristics were as follows: pH (H_2O)=6.9, EC=0.18 mS cm^{-1}, sand=14%, silt=49%, clay=37%, organic matter=1.4%, total *N*=1.03 g kg^{-1}, assimilable *P*=42 mg kg^{-1}, exchangeable *K*=108 mg kg^{-1}.

The dynamic fertigation strategies presented until now allow the individuation of the optimal timing to supply N fertilizers, but little information is provided about the optimal N rate to be supplied. In dynamic N strategies, the N rate to be supplied at each fertigation is calculated to provide the amount of the nutrient needed to sustain the growth until the next monitoring with the radiometer, typically conducted every 7–10 days. The N rate at each fertigation was calculated considering the expected daily N uptake, which was derived after the computation of the N balance sheet method (Gianquinto et al. 2011b) according to Eq. (2):

$$\text{N rate}\ \left(kg\ N\ ha^{-1}\right) = N_r + N_l + N_v - N_{SOM} - N_s - N_{pc} - N_{iw} \quad (2)$$

Where N_r is the crop N requirement considering the critical N uptake of 2.24 kg N t^{-1} of marketable yield (Tei et al. 2002) and 110 t ha^{-1} as expected yield, N_l is the N leached, N_v the N volatilized through denitrification as N_2O, N_{SOM} the N mineralized from soil organic matter (estimated as a function of C/N, soil texture, and soil organic matter as recommended by regional technical recommendation Emilia-Romagna, 2022), N_s the N present in the soil determined with laboratory analysis, N_{pc} the N provided from the previous crop (winter wheat) and N_{iw} is the N supplied from the irrigation water. The estimated total crop N rate, according to the N balance sheet, was 180 kg N ha^{-1}.

The daily N uptake rate was estimated by Tei et al. (2015), considering that 6% of the total N uptake (about 11 kg N ha^{-1}) is absorbed by the crop from 0 DAT to 28 DAT, 78% (about 140 kg N ha^{-1}) from 29 to 77 DAT, and 16 % from 78 to 105 DAT (about 29 kg N ha^{-1}). Therefore, the daily N uptake was easily calculated for each growth stage (0.39, 2.85, and 1.07 kg N ha^{-1} d^{-1}, respectively).

Five N-management strategies were tested:

- Fertilized control (N180), where 180 kg N ha^{-1} (ammonium nitrate, NH_4NO_3, *N*=34%) was supplied via fertigation split into 7 applications following the daily N uptake rate of processing tomato. This was used as a spy plot.
- N SPY, where N fertilizers were supplied whenever the SI (see Eq. (1)) was lower than 0.9.
- N THR, where N fertilizers were supplied whenever the GVI was below the fitted threshold curve reduced by 10%. The GVI threshold curve adopted for Exp. 2 was different from the one adopted in Exp. 1, as will be specified in Section 2.3.
- N THR_{N30}, like N THR but the N application rate calculated through the expected daily N uptake was reduced by 30% after a fertigation was recommended.
- N SPY_{EVO}, where N was supplied whenever the GVI monitored was below 90% of the GVI profile of a spy plot of the same cultivar (K2206), retrieved from the same location of the previous year (2022) and fertilized with 180 kg N ha^{-1}, just as in the well-fertilized control in the current experiment (further details on the experiment are available in Cerasola et al. 2023). This strategy is conceptually similar to N SPY but does not need the simultaneous presence of the well-fertilized spy plot in the field. Therefore, it was named EVO (*evolved*).

In dynamic N strategies of Exp. 2, 10 kg N ha^{-1} were supplied through fertigation 7 days after the transplant as a starter dose. In all the experiments, water soil moisture was maintained at the field capacity with drip irrigation through the water balance sheet method according to the guidelines proposed by FAO Paper 56 (Allen et al., 1998; Cerasola et al.

2022). Crop evapotranspiration was calculated through the Hargreaves-Samani formula (Hargreaves and Samani 1985), adopting the single K_c. If one treatment needed to be fertilized through fertigation, the same amount of water was supplied to the other experimental treatments to ensure the same soil moisture.

2.2. Spectral reflectance monitoring

Two different passive multispectral radiometers were used in this study: the Multispectral Radiometer MSR5/87/16R (CropScan, Inc. Rochester, MN, USA) and the Spectrosense 2+ (Skye Instruments, Llandrindod Wells, UK), for Exp. 1 and 2, respectively. The two instruments have similar technical features, both with a full-width half maximum (FWHM) of 10 nm at *p560* and *p810* nm.

The GVI used to guide the N fertilization in all the experiments was calculated as follows (Eq. (3)):

$$GVI = \frac{p810}{p560} \tag{3}$$

Where *p810* is the crop reflectance in the near-infrared (NIR) at 810 nm, and *p560* is the crop reflectance in the green region at 560 nm.

In both experiments, the GVI was monitored once or twice a week in three sampling areas of about 0.6 m^2 per experimental plot. The measurements were carried out on sunny days with incident radiation around the zenith between 11.00 am and 2.00 pm, with the instrument placed 1.80 m above the canopy (Gianquinto et al. 2019).

2.3. The critical thresholds of GVI

The critical threshold curves of GVI adopted for managing dynamic N treatments are derived from the interpolation of GVI data along the GDDs. GDDs were calculated considering 8 and 30 °C as basal and maximum temperatures, respectively (Incrocci et al. 2020). However, the GVI threshold curves adopted in Exp. 1 and Exp. 2 were different. In Exp. 1, the critical curve adopted was developed as indicated in Gianquinto et al. (2004), following a linear-plateau interpolation. Briefly, the GVI was monitored in processing tomato plants in a silty loam soil held in Legnaro (Padova, Italy) in 2002, and in Rosolina (Rovigo, Italy) in 2003, including different N rates in a complete randomized block design (further details on the experiment available in Gianquinto et al. 2011a). At harvest, the relative yield (Y_r) was calculated as the ratio between the yield of the experimental plot and the maximum yield observed within the same block. Hence, the GVI was monitored at different moments of the growing season. Subsequently, the critical GVI (GVI_c) value (i.e., the minimum value of GVI that maximizes the yield in that specific growth stage, Fig. 1a) was derived from a linear-plateau model with the relative yield, defined in Eq. (4):

$$Y_r = \begin{cases} a\,GVI + b, & GVI < GVI_c \\ c, & GVI \geq GVI_c \end{cases} \tag{4}$$

Where *a* and *b* are the slope and intercept, and *c* is the plateau of the linear-plateau model. At each growth stage indicated by the GDDs, the GVI_c is derived (Supplementary material S1 and S2). The obtained GVI_c were interpolated with the GDDs in a second-order polynomial function (Fig. 1b).

In Exp. 2, in addition to the GVI_c developed for Exp. 1 (Fig. 1b),

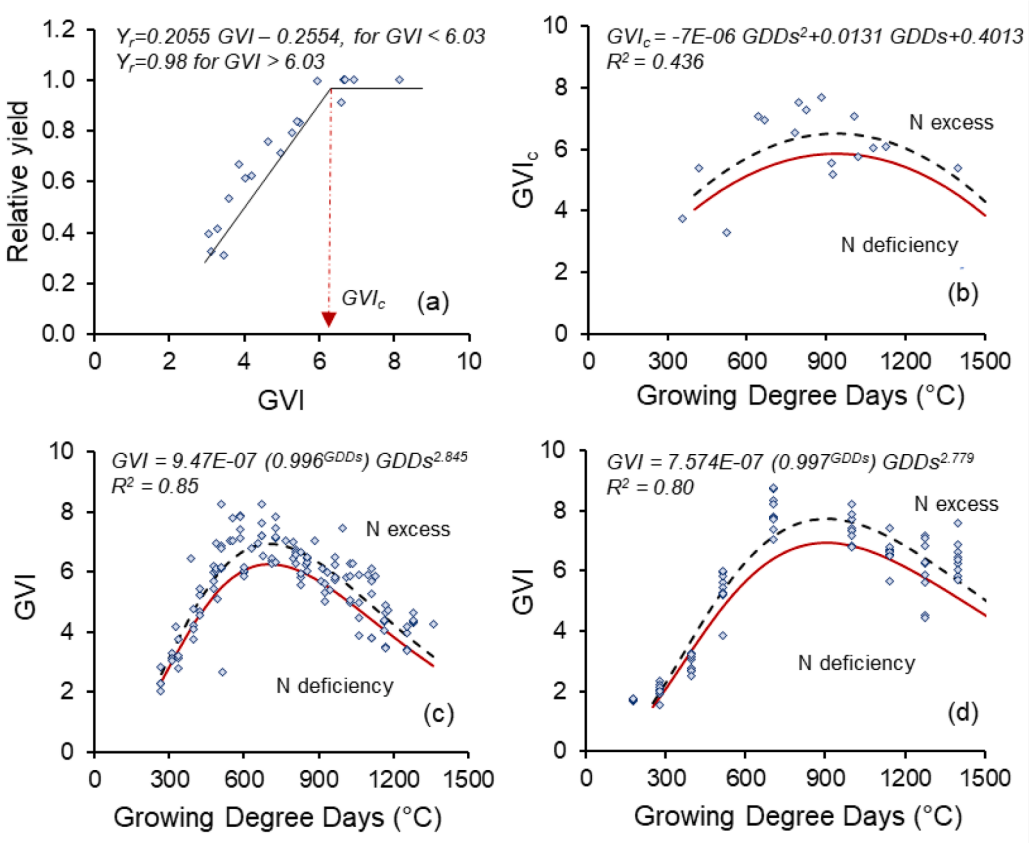

Fig. 1. Linear-plateau relationship between the GVI and relative yield at 932 growing degree days (GDDs) (a). The GVI_c were then used to develop the GVI_c threshold curve along GDDs (b) used in Exp. 1 (n=16). The Hoerl models adopted as GVI threshold curve for N THR and N THR_{N30} treatment (c, n=124) and for N SPY_{EVO} treatment (d, n=78) in Exp. 2 are reported. The black dashed lines represent the threshold curve resulting from the fitting procedure, while the red lines represent the threshold curve reduced by 10%, used to trigger the fertigation.

further GVI data were included in the threshold model, which were collected in processing tomato cultivation grown in a commercial farm in Codigoro (Ferrara, Italy 44°50′N 12°07′E, 3 m a.s.l.), thus maintained under non-limiting N status by the farmer. Different growing seasons (2004 and 2005), and cultivars (Jet, Precocix, and UGX 822) were included. Therefore, the GVI data monitored under field conditions were pooled with the GVI_c, and the software CurveExpert Basic (version 2.2) was used to interpolate the data to find the best-fitting model. The Hoerl model, a curve asymmetric concerning the maximum point that fits well with the arrangement of data already observed in similar studies (Rajarathinam and Vetriselvi 2017; Mariotti et al. 2018), was adopted and described in Eq. (5):

$$GVI = ab^{GDDs}GDDs^{c} \quad (5)$$

Where *a, b,* and *c* are the Hoerl models' coefficients, and GDDs are the growing degree days (Fig. 1c).

In Exp. 2, the N SPY_{EVO} was managed using the GVI profile along the GDDs monitored in a well-fertilized plot (spy plot that received 180 kg N ha^{-1}) in an experiment realized in the previous year in the same location and under the same growing conditions (2022, Cerasola et al. 2023). The obtained GVI data were interpolated with a Hoerl model along the GDDs (Fig. 1d).

2.4. Yield determination, physiological measurements, and efficiency indices

Quantitative, qualitative, and physiological measurements were taken and resumed in Table 2. Quantitative and qualitative measurements were taken at the harvest that occurred at 107, and 100 DAT for Exp. 1 and Exp. 2 respectively (1450 and 1670 °C of GDDs, respectively for Exp. 1 and Exp. 2). At harvest, 8 plants per experimental plot were harvested in both experiments excluding border plants to mitigate the border effect. After plant harvest, fruits were partitioned, as indicated in Table 2, into ripe and healthy, partially ripe, green, sunburned, with minor or deep lesions, rotten, and with blossom end rot (BER). Total and marketable yield (t ha^{-1}) were derived, and the harvest index was calculated in Exp. 2 as the ratio between the commercial yield and the total biomass (green biomass and total fruit yield).

In Exp. 2, photosynthesis measurements were taken at 67 DAT with the Li-COR 6400 (Lincoln NE, USA). Measurements were taken between 9.00 and 11.00 am, in one sun-exposed leaf of three plants per plot, which were averaged to obtain a single value per experimental plot. Assimilation rate (A, μmol CO_2 m^{-2} s^{-1}), transpiration rate (E_{mm}, mmol H_2O m^{-2} s^{-1}), and stomatal conductance (g_{sw}, mol H_2O m^{-2} s^{-1}) were measured. Water use efficiency at the leaf level (WUE_L, μmol CO_2 $mmol^{-1}$ H_2O) was calculated as the ratio between the assimilation rate and the transpiration rate (Medrano et al. 2015).

In addition to saving N fertilizers in dynamic strategies compared to the well-fertilized control (% of N saved), the Nitrogen Use Efficiency (NUE) and fertilization costs were calculated as agronomic and economic performance indicators. The NUE was calculated as the ratio between the marketable yield obtained and the N input used (t kg^{-1} N). Regarding the fertilization costs, the price of urea in May 2024 (285 $ t^{-1}) was derived from the World Bank (2024), and the price per kg of N supplied was calculated considering the N content (*N*=46%) and converted to euros (€), resulting in 0.574 € kg^{-1} N. The fertilization costs were calculated for both experiments and expressed in relation to the marketable yield (€ t^{-1} of marketable yield).

Table 2
Quantitative, qualitative, and physiological determinations in the three experiments.

	Exp. 1	Exp. 2
Quantitative measurements		
Fruit number	X	X
Average fruit weight	X	X
Healthy and ripe fruits	X	
Sunburned fruits	X	
Green fruits	X	X
Fruits with deep lesions	X	
Fruits with minor lesions	X	
Rotten fruits	X	
Fruits with BER		X
Marketable yield	X	X
Total yield	X	X
Harvest index		X
Qualitative measurements		
pH	X	X
EC	X	
Brix	X	X
Dry matter content	X	X
Lycopene		X
Physiological measurements		
Photosyntesis and transpiration		X

2.5. Fruit quality

Fruits were selected from the marketable fraction for quality trait determination. pH and EC were monitored through portable meters (Hanna Instruments, Padova, Italy), as well as for the Brix degree (PAL-1 Atago, Tokyo, Japan). Dry matter content was determined after oven-drying tomato fruits at 65 °C until constant weight. Regarding lycopene determination, approximately 300 g of fresh fruit were randomly selected from the marketable yield and thoroughly ground with an immersion blender and frozen at −20 °C until lycopene extraction. The extraction of lycopene and analysis protocol was adapted from Appolloni et al. (2023) and is detailed in the supplementary materials (S3).

2.6. Greenhouse gas emissions assessment

An environmental assessment was conducted to quantify the greenhouse gas (GHG) emissions related to the different N management strategies. First, the emissions of N_2O from the soils because of N fertilizer application from the different N management strategies were quantified considering the International Panel on Climate Change (IPCC) guidelines (Hergoualc'h et al. 2019). In our assessment, only the direct and indirect emissions related to synthetic N fertilizers applied were considered. Drip irrigation system accounts for a lower N_2O emission compared to other systems (e.g., furrow, or sprinkler irrigation), therefore, direct N_2O emissions from soil after the application of N fertilizers were quantified specifically for the drip irrigated system, as suggested by Kuang et al. (2021) and reported in Eq. (6).

$$Direct\ N_2O\ \left(kg\ N_2O\ ha^{-1}year^{-1}\right) = 0.6696 + 0.001 \cdot N(1.11903 + 0.009362 \cdot N) \cdot \frac{44}{28} \quad (6)$$

Where N is the amount of N fertilizers used with the different N management strategies, and 44/28 is a conversion factor to convert the kg N_2O—N into kg N_2O (Hergoulac'h et al. 2019).

However, the N present in soil also undergoes volatilization in the form of ammonia (NH_3) and NO_x, and these gases and their products (NO_3^- and NH_4^+) deposit back into soil and water (Hergoualc'h et al. 2019). From here, N is re-emitted in the form of N_2O. This indirect pathway was considered as well in the accounting process and quantified as reported in Eq. (7):

$$Indirect\ N_2O\ \left(kg\ N_2O\ ha^{-1}year^{-1}\right) = N \cdot Frac_{GASF} \cdot EF \cdot \frac{44}{28} \quad (7)$$

Where $Frac_{GASF}$ is the fraction of N fertilizers that volatilize as NH_3 and NO_x (set at 0.1), and EF is the Emission Factor for N_2O emissions from atmospheric deposition of N on soils and water surfaces, and set at

0.01 (Hergoulac'h et al. 2019).

Then, the total GHG emissions were calculated by converting the total N_2O emissions (direct+indirect) into CO_2eq by multiplication for the conversion factor 265 (Menegat et al. 2022). N leaching and N runoff were omitted, as they are negligible in drip-irrigated cultivation systems (Hergoulac'h et al. 2019).

In addition, the CO_2eq emissions associated with industrial fertilizers manufacturing (*Fm*) were included in the assessment, assuming that the best environmentally friendly technology is adopted in the production system, emitting 3.6 t CO_2eq t^{-1} N produced (HESQ and Fossum 2014). The GHG intensity (kg CO_2eq t^{-1} $year^{-1}$) was calculated considering the ton of product as a functional unit (Ruan et al. 2024) as reported in Eq. (8):

$$GHG\ intensity = \frac{(Direct\ N_2O + Indirect\ N_2O)\cdot 265\ +\ Fm}{Yield} \quad (8)$$

2.7. Statistical analysis

The linear-plateau models were generated with RStudio (ver. 4.2.2, packages *nlstool,* Baty et al. 2015, and *nlraa,* Miguez 2022), while the quadratic interpolation (Fig. 1b) was carried out in Excel. For models reported in Fig 1c and 1d, the fitting procedure was supported by the CurveExpert Basic software (version 2.2) to select the best fitting model. Data generated from the trials were analyzed with one-way ANOVA in RStudio (version 4.2.2, packages *car*, Fox and Weisberg 2018, and *emmeans*, Lenth 2022), and normality and homoscedasticity were checked respectively with the Shapiro-Wilk and the Levene test. The Tukey test was adopted to separate the marginal means. In case such assumptions were not met, the non-parametric Kruskal-Wallis test was adopted, and the Dunn test with Bonferroni correction was used to separate the medians.

3. Results

3.1. Climate along the growing seasons

The climate data monitored during the experiments are shown in Table 3. Because of the higher temperature observed in Exp. 2, the harvest occurred at 1674 GDDs (Table 3). The daily GDDs accumulated by the crop were, therefore, +24 % higher in comparison with the daily GDDs accumulated during Exp. 1 (Table 3). Also, the cumulative ET_0 computed along Exp. 2 was the highest due to the higher temperatures monitored. The high ET_0 during Exp. 2 was exacerbated by the reduced rainfalls that occurred during the growing season, which made the meteorological conditions warmer and drier compared to Exp. 1.

3.2. Impact of dynamic N strategies on time course of GVI, yield, efficiency of N fertilization and photosynthesis

In Exp. 1, the pattern of the GVI along the GDDs is shown in Fig. 2 for each N management strategy. Coherently with the N supply, N0 experienced the lowest GVI value during the growing season, even below the threshold curve, confirming its response to soil N availability. The GVI of N180 sharply increased above the threshold curve up to a value of 8, resulting to be the highest in comparison to the other experimental

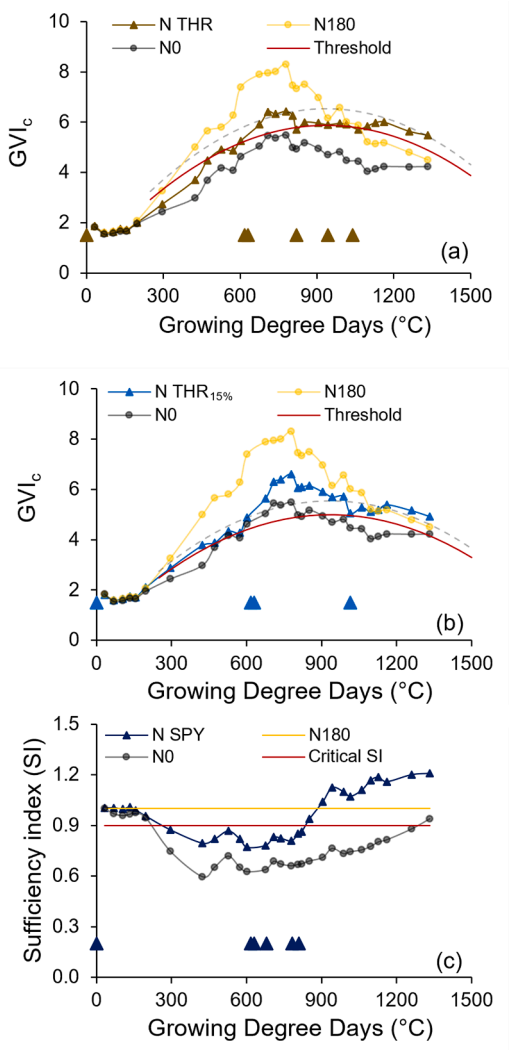

Fig. 2. Pattern of the GVI as a result of the dynamic N management strategies in Exp. 1. The dashed grey lines in a and b represent the threshold curve obtained from the fitting procedure. In contrast, the red lines represent the threshold used to trigger the N fertigation. In c, the sufficiency index (SI) pattern as a result of the management according to the N SPY is represented, and the red line represents the minimum limit of the sufficiency index to trigger the N fertigation set at 0.9. The larger triangles (▲) represent an application of N through fertigation. The first ▲ at 0 GDDs represents the application of N in pre-transplant with solid urea at 30 kg N ha^{-1}.

treatments until 900–1100 GDDs (Fig. 2), which then sharply decreased below the threshold curve in Fig. 2a. Whenever the GVI of N THR or N $THR_{15\%}$ was below the respective threshold curve, the N fertilizer was supplied via fertigation, resulting in 5 and 3 fertigations respectively (Fig. 2a and 2b). The sufficiency index of the N SPY induced 5 fertigations along the growing season. Then the SI was above 1, meaning that the GVI of the N SPY was higher than the GVI of N180 in the last part of

Table 3
Climate data monitored across the experiments. GDDs stands for Growing Degree Days, while ET_0 is the potential evapotranspiration calculated according to the Hargreaves-Samani equation. The daily GDDs were calculated considering the GDDs at harvest and the length of the growing season in days.

		°C			°C	°C	mm	mm
	Transplant date	Air temperature			GDDs at harvest	Daily GDDs	Cumulative rainfall	Cumulative ET_0
		Min	Max	Med				
Exp. 1	11 May 2004	15.8	27.1	21.4	1450	13.6	203	526
Exp. 2	24 May 2023	17.7	31.2	24.5	1674	16.7	94.7	575

the growing season.

The dynamic N strategies resulted in a lower N supply than N180 (N $THR_{15\%}$, N THR, and N SPY supplied 60, 92, and 114 kg N ha^{-1}). Still, no significant differences were detected among the marketable yield (Fig. 3a). Significant differences were observed in marketable yield only for the non-fertilized control, which resulted to be the lowest compared with the fertilized N strategies (Fig. 3a). A linear-plateau model was interpolated between the N supply and the marketable yield (Fig. 3a), and the critical N supply was found to be 81.6 kg N ha^{-1}. Maintaining high marketable yields with a reduced application of N fertilizers significantly increased the NUE in dynamic N strategies compared to the N180 (Fig. 3b). Among the dynamic N strategies, the highest NUE was observed for N $THR_{15\%}$, while the lowest was observed for N SPY, which is consistent with the N saving (Fig. 3b). This positively impacted the fertilization costs, where the most cost-effective strategies were the N THR and N $THR_{15\%}$ with 0.39 € t^{-1} of marketable yield, compared to the fertilized control (N180) that reached 0.93 € t^{-1} of marketable yield (Fig. 3c).

In Exp. 2, different GVI threshold models were adopted (Fig. 4). It is worth noting that the GVI profile of N180 did not precisely align with the threshold model, and a slight rightward shift was observed (Fig. 4a). Notwithstanding, this did not deplete the performances of the N THR and N THR_{N30}. Indeed, a reduced amount of N was supplied with the N THR and N THR_{N30} (Table 4), with four and five fertigations, respectively (Fig. 4a), compared to the N180, and a comparable yield was obtained (Table 4). Conversely, a better overlap of the N180 was observed with the EVO model (N SPY_{EVO}) (Fig. 4b). Similar performances were observed for the N SPY_{EVO}, where 71 kg N ha^{-1} were supplied (Table 4) in four fertigations (Fig. 4b) without significant yield reduction. All these dynamic N strategies determined the lowest N supply with savings ranging from 56 to 60%, thus exhibiting the highest NUE (Table 4). This is also reflected in the lowest fertilization costs (Table 4). Reduced performances in terms of NUE were observed for the

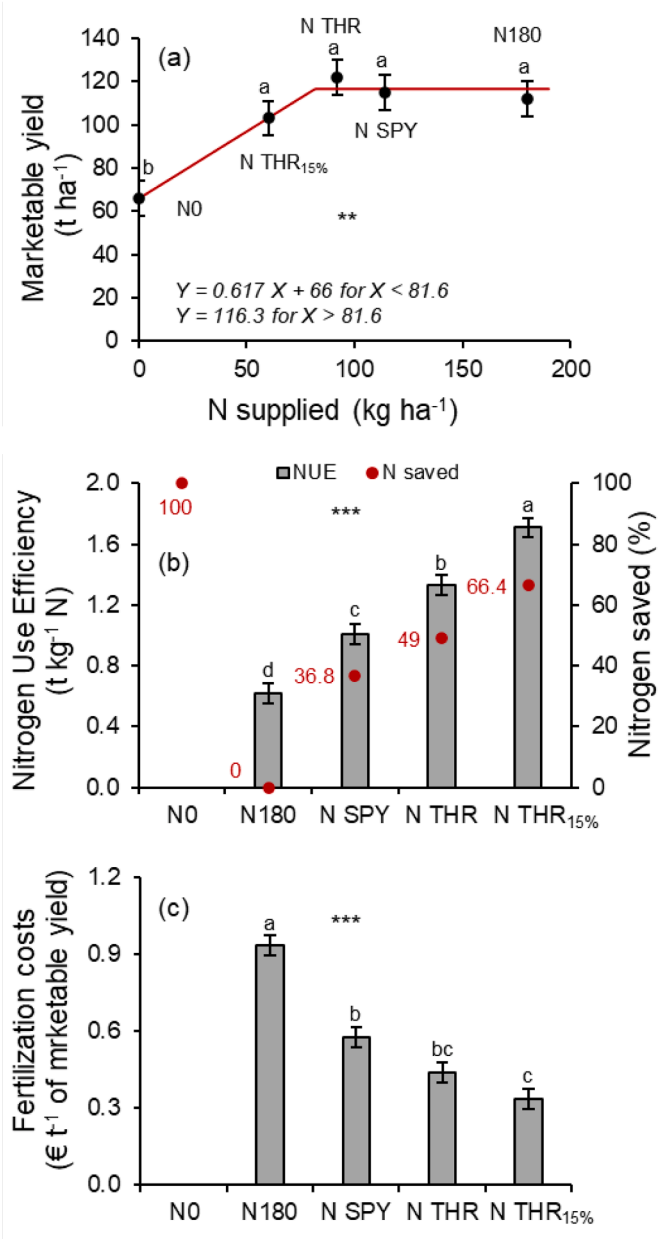

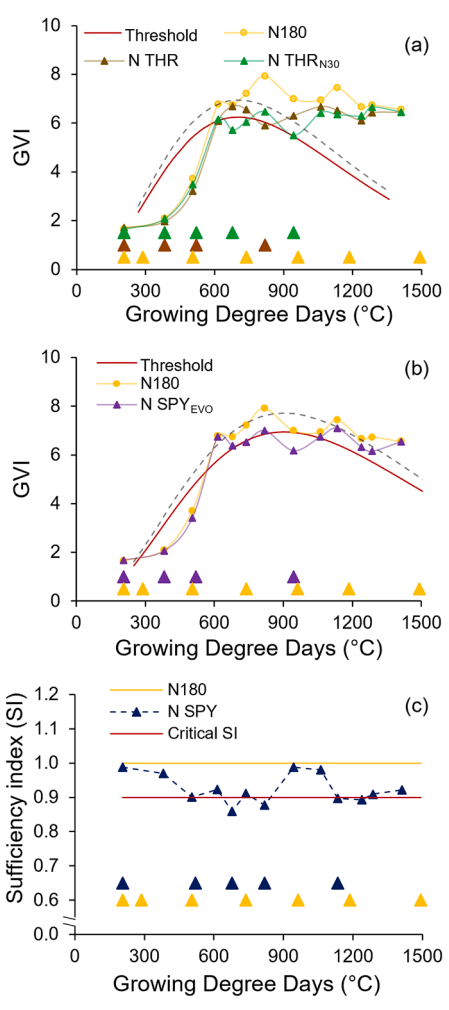

Fig. 3. Impact of different N management strategies in Exp. 1 on marketable yield (a). Data were fitted with a linear-plateau model (red line), which resulted significant for $p < 0.05$. In b, the effect of N management strategies on N saved, and NUE is also shown. The NUE of N0 treatment is not calculated. c represents the fertilization costs. The values are the average of four replicates. Different letters indicate significant differences at ANOVA (*** for $p < 0.001$, ** for $p < 0.01$), while vertical bars represent the standard error.

Fig. 4. Pattern of the GVI as a result of the dynamic N management strategies in Exp. 2. The dashed grey lines in a and b represent the threshold curve obtained from the fitting procedure. In contrast, the red lines represent the GVI threshold curves specific for the N THR strategies (a) and N SPY_{EVO} strategy (b) reduced by 10%. In c, the red line represents the minimum limit of the sufficiency index (SI) to trigger the N fertilization in N SPY treatment set at 0.9. The triangles (▲) represent a fertigation of N according to the management strategy.

Table 4
Impact of dynamic N management strategies on yield, N inputs, and Nitrogen Use Efficiency (NUE) of Exp. 2. Values are the average of four replicates, SE indicates the standard error, ns indicates "not significant", "-" indicates that the ANOVA was not performed, while different letters indicate significant differences at ANOVA at $p < 0.001$ (***).

		N180	N SPY	N THR	N THR_{N30}	N SPY_{EVO}	SE	
Marketable yield	*t ha^{-1}*	124^{a}	121^{a}	124^{a}	106^{a}	120^{a}	5.71	ns
N applied	*kg ha^{-1}*	180	112	80	73	71	–	–
N saved	*%*	0	38	56	59	60	–	–
NUE	*t kg^{-1}* N	0.69^{c}	1.08^{b}	1.55^{a}	1.45^{a}	1.68^{a}	0.058	***
Fertilization costs	*€ t^{-1}*	0.84^{a}	0.59^{b}	0.37^{c}	0.39^{c}	0.34^{c}	0.028	***

N SPY treatment in comparison with the formers dynamic N strategies, but still improved as compared with the fertilized control N180 (Table 4), confirming the same result obtained in Exp. 1 (Fig. 3b). Harvest index was not significantly affected by the N strategy, although the low p-value (0.08, see Supplementary material S4) may suggest that further investigation is still needed. Although the biomass was measured only at the harvest, the dynamic N strategies exhibited visibly reduced biomass compared with N180 during the vegetative growth.

Significant differences were detected in total and marketable fruit numbers in both experiments (Fig. 5), where the lowest fruit number was observed in dynamic N strategies in both experiments (Fig. 5a, 5b). In Exp. 1, the lowest fruit number was observed for N0, the highest for N180, and intermediate fruit numbers were observed for the dynamic strategies (Fig. 5b). In Exp. 2, the highest fruit number was observed for N180, the lowest in N SPY, N THR and N THR_{N30}, whereas N SPY_{EVO} showed fruit numbers not significantly different from N180 and the former dynamic strategies (Fig. 5a). On the other hand, fruit weight was increased by dynamic N strategies, but only in Exp. 1 (Fig. 5c).

In Exp. 1, dynamic N strategies did not affect green fruit incidence, deep or minor lesions, or blossom end rot (Supplementary material, S3). However, dynamic N strategies significantly improved the fraction of healthy and ripe fruits, and reduced the incidence of sunburned fruits, compared to N180 (Fig. 5d). N THR accounted for the lowest incidence of rotten fruits, while the highest incidence was observed for N180. N0, N SPY and N $THR_{15\%}$ showed an incidence of rotten fruits not significantly different from N180 and N THR. Crop photosynthesis and transpiration parameters (E_{mm} and g_{sw}) at the leaf scale were not influenced by dynamic N management strategies (Table 5).

3.3. Fruit quality

Among the fruit quality parameters, no significant differences were

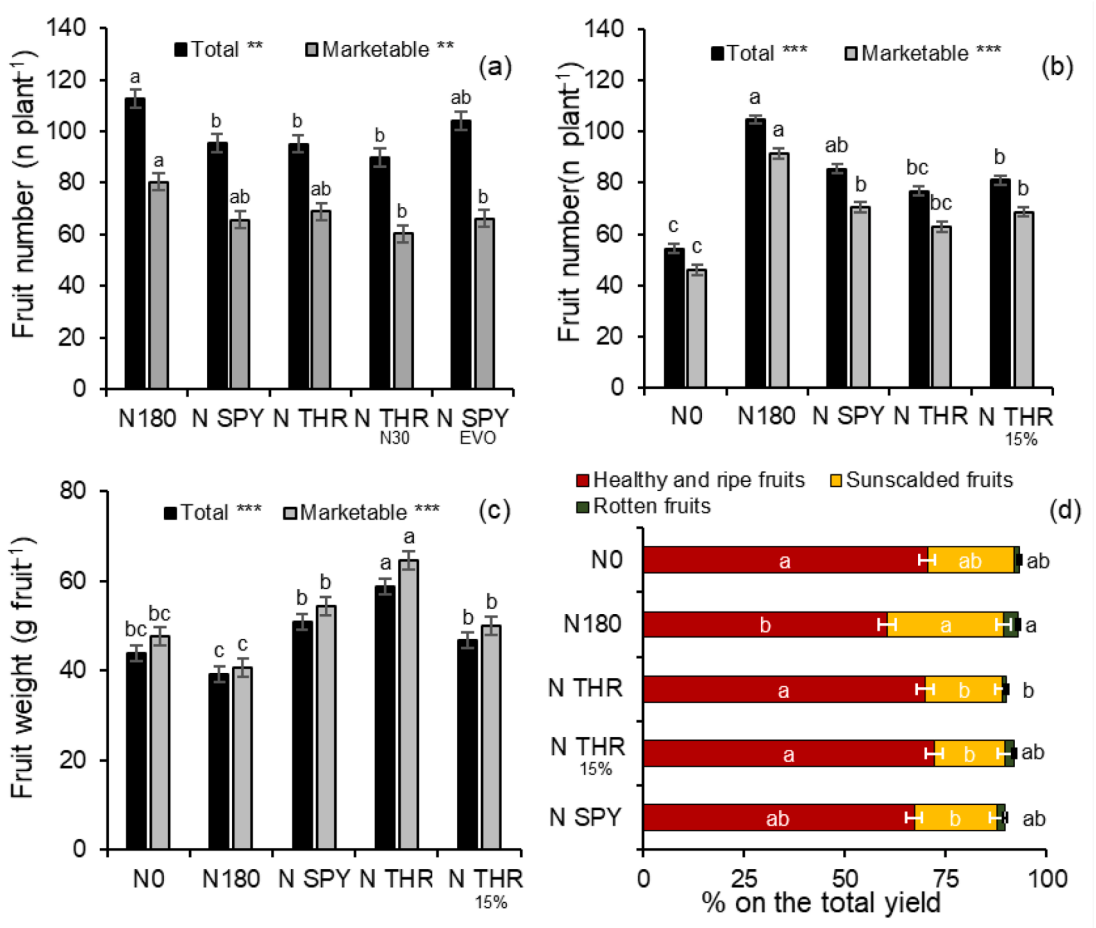

Fig. 5. Effect of dynamic N strategies on fruit number (a in Exp. 2 and b in Exp. 1) and fruit weight (c) in Exp. 1. The impact of N management strategies on fruit yield composition in Exp. 1 is also shown (d). The bar value is the average of four replicates. Different letters indicate significant differences between bars with the same color. at $p < 0.001$ (***) and $p < 0.01$ (**), while vertical and horizontal bars represent the standard error.

Table 5
Physiological traits monitored in Exp. 2 at 67 DAT. (*) indicate a non-normal distribution. Therefore, the Kruskal-Wallis test was used to check differences for (*), and the median is reported instead of the average of the four replicates. SE stands for standard error, while "ns" stands for not significant.

	$A^{(*)}$ µmol m^{-2} s^{-1}	E_{mm} mmol m^{-2} s^{-1}	$g_{sw}^{(*)}$ mol m^{-2} s^{-1}	WUE_L µmol CO_2 $mmol^{-1}$ H_2O
N180	15.1	9.38	0.665	1.62
N SPY	16.9	9.90	0.675	1.88
N THR	16.7	9.33	0.662	1.84
N THR_{N30}	17.0	9.35	0.667	1.82
N SPY_{EVO}	16.6	9.46	0.670	1.68
SE	1.00	0.19	0.019	0.082
Significance	ns	ns	ns	ns

detected in the pH and EC of the fruit juice, nor the dry matter content (Supplementary material, S5). In Exp. 2, lycopene ranged 96 to 122 mg kg^{-1} fresh weight, but no significant difference was detected ($p = 0.09$). However, the soluble solids content (°Brix) was affected by experimental treatments in Exp. 2, as it was the highest in dynamic N strategies compared to the N180 control (Fig. 6). Among the dynamic N strategies, N SPY_{EVO}, N THR, and N THR_{N30} were the best-performing strategies for sugar accumulation in fruits (+10.4% as compared with N180), while N SPY yielded a lower value of °Brix among the dynamic strategies, but still higher compared to N180 (Fig. 6).

3.4. Greenhouse gas emissions

GHG emissions intensity was calculated per t of product as a functional unit and was significantly affected by the N strategies in both experiments (Fig. 7), with the highest GHG emissions intensity observed for N180. In Exp. 1, the lowest GHG emissions were observed, as expected, for N0. At the same time, N THR, N $THR_{15\%}$, and N SPY were all significantly different from N180 (Fig. 7a). Furthermore, non-significant differences were observed between N $THR_{15\%}$ and the non-fertilized control N0. In Exp. 2, N THR, N THR_{N30} and N SPY_{EVO} were the most efficient dynamic N strategies in terms of GHG emissions, while higher emissions were estimated for N SPY, but still lower than the fertilized control (Fig. 7b). The highest impact in emissions associated with N fertilization is observed for the manufacturing stage (54% of total GHG emission), and direct N_2O emissions (41% of total GHG emissions). On average, the dynamic N management strategies reduced the GHG intensity by about 46% in Exp. 1, and 44% in Exp. 2 compared to the fertilized control.

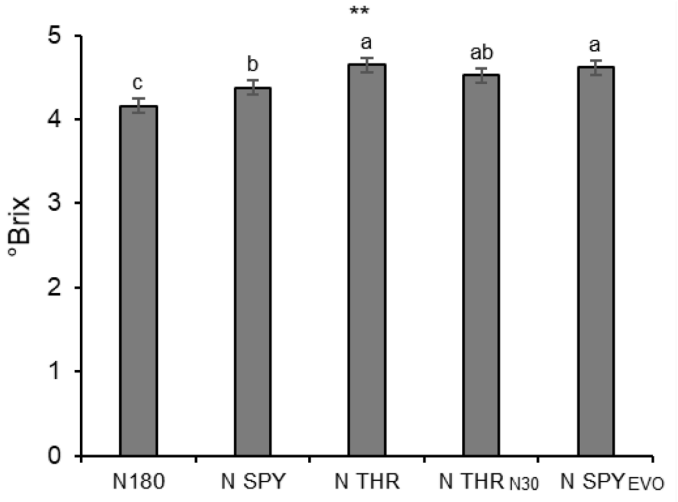

Fig. 6. °Brix as affected by the dynamic N management strategies. The bar value is the average of four replicates. Different letters indicate significant differences at $p < 0.01$ (**), and vertical bars represent the standard error.

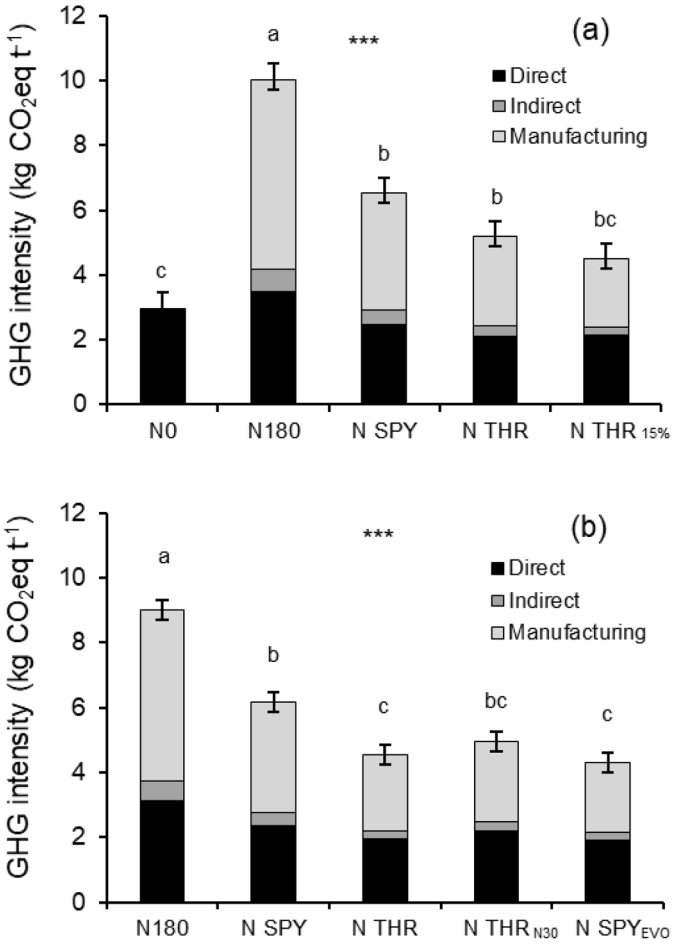

Fig. 7. Greenhouse gase (GHG) emissions associated with the N fertilization of the different N management strategies in Exp. 1 (a) and Exp. 2 (b). The bar value is the average of four replicates. Different letters indicate significant differences at $p < 0.001$ (***), and vertical bars represent standard errors.

4. Discussion

4.1. Impact of dynamic N strategies on fertilization efficiency, physiology, and yield

The frequent overuse of N fertilizers is among the main reasons for the tomato environmental burden at the cultivation stage (Ronga et al. 2019a). Therefore, developing new strategies aimed at optimizing N fertilizer supply is of pivotal importance. The European Farm to Fork Strategy (European Commission 2020) aims to reduce by 20% the use of fertilizers by 2030. In this study, we demonstrated that a dynamic N strategy using multispectral reflectance sensors allowed for a significant saving in N fertilizer supply by 37 to 60% (a reduction in measure of 68 to 120 kg N ha^{-1}, see Fig. 3b and Table 4) compared to the control fertilization level (180 kg N ha^{-1}), well above the target objective of EU. Coherently with our findings, dynamic N strategies were effective in reducing N fertilizers in cantaloupe by 17–66% (Gianquinto et al. 2010) and in tutored tomato by 25–44% (Oliveira et al. 2019) using the spy plot strategy, and in potato by 37–58% using SPAD threshold values (Gianquinto et al. 2001). In Exp. 1, a linear-plateau regression model was developed between the N supply of the different management strategies and the yield response, revealing an optimal N supply at around 80 kg N ha^{-1} (Fig. 3a). This is significantly lower when compared

to the optimal N rate suggested by former authors in drip-fertigated processing tomatoes in a Mediterranean environment, ranging 160 to 200 kg ha^{-1} (Erdal et al. 2006; Ronga et al. 2019b; Hartz and Bottom 2009). The N THR strategies (N THR, N $THR_{15\%}$, N THR_{N30}) and N SPY_{EVO} supplied an amount of N fertilizers between 60 and 90 kg ha^{-1} (75 kg N ha^{-1} on average), close to the optimal N dose (Fig. 3a, Table 4), meaning that these strategies are effective in maintaining the crop within the optimal N status avoiding yield losses (Gianquinto et al. 2001), and overall maximizing the NUE. N SPY strategy supplied the highest amount of N fertilizer among dynamic treatments, around 115 kg N ha^{-1} in both experiments, but still lower than the fertilized control N180 (Fig. 3a, Table 4). Although the N SPY strategy significantly improved the NUE (Gianquinto et al. 2010), it was less efficient among the dynamic N strategies (Fig. 3b, Table 4). Using an over-fertilized control (N180) as a reference to trigger N fertilization could have led to a supply of N when it was not required by the crop. Therefore, reducing the threshold of the sufficiency index from 0.90 (as adopted in this work) to 0.80–0.85 to trigger N fertilization may further optimize the N SPY strategy. Notwithstanding, the adoption of the N SPY strategy in field conditions is limited by logistical constraints, e.g., splitting the irrigation system into two independent modules or identifying a representative window of the field (Gianquinto et al. 2004). Adopting absolute threshold GVI values (e.g., Fig. 1b, 1c, 1d) would solve this issue, and their adoption by farmers could be sped up. In economic terms, dynamic N management strategies (N THR strategies, and N SPY_{EVO}) allowed to reduce the fertilizers costs per t of marketable yield by around 57% without yield losses (Table 4), which is of utmost significance considering that the prices of urea are heavily affected by the geopolitical scenario (Valenzuela 2024), reaching the maximum peak in April 2022 at 0.85 € kg^{-1} (recalculated from World Bank 2024). However, a more detailed economic analysis should be carried out considering not only the savings in N fertilizer use but also the technology adopted (e.g., time taken for the monitoring and amortization of the costs of the reflectance sensor). If open-access satellites are used (e.g., Sentinel 2, with a spatial resolution of 10 m x 10 m for the monitoring of GVI), then the costs of the technology can be minimized.

In Exp. 1, the N rate to be supplied in dynamic management was not based on strict criteria, and only a small amount of N was supplied whenever the GVI fell below the reference value of the respective management strategy (ranging from 10–25 kg N ha^{-1}, based on crop phenological stage). In Exp. 2, the N rate to be supplied was based on the N balance computation, providing a better theoretical framework to support the definition of the N rate. Here, a reduction of 30% of the computed N rate was included in the N THR_{N30} strategy to validate the effectiveness of this approach in defining the optimal N rate. The N THR_{N30} strategy reduced the total N supply of a negligible amount of 7 kg N ha^{-1} compared to the N THR strategy (Table 4), requiring a higher number of fertigations (five vs four of N THR). This evidence suggests that reducing the N supply by 30% in the N THR strategy, leads more frequently to N deficiency conditions, inducing more frequent N supplies without significant N saving compared to N THR. Therefore, defining the N rate based on the integration of N balance computation with the dynamic N strategies is a suitable approach for processing tomatoes. However, some limitations must be highlighted when adopting the N balance. First, its computation relies on estimating the expected yield that will be obtained at the harvest, which is a matter of wide debate among the scientific community (Ravier et al. 2016). Secondly, the difficulties in estimating the parameters needed to compute the N balance (e.g., N mineralization, N leaching, crop N uptake, and so forth) made it an obsolete tool, according to Ravier et al. (2016). Thus, innovative approaches are needed to compute the N rate based on the integration of crop models with reflectance (see Cerasola et al. 2025, Li et al. 2022a and Houles et al. 2007 for details).

It is also noteworthy that the pattern of the GVI of N180 in Exp. 2 did not fully overlap with the THR model, especially in the first stages of the growing season (Fig. 4b). In Exp. 2, a different cultivar was adopted than those used to develop the THR model, therefore we hypothesize the presence of cultivar effects (Pinter et al. 1985). While some authors found negligible (Padilla et al. 2024) or absent (De Souza et al., 2020) differences in reflectance of different cultivars of muskmelon and sweet pepper, Crusiol et al. (2017) found that NDVI can differentiate soybean cultivars only under drought stress. Conversely, Gianquinto et al. (2019) found that processing tomato cultivars can significantly affect the GVI monitoring, suggesting that the impact of cultivars in vegetation index monitoring could be species-specific. In contrast, the threshold model N SPY_{EVO}, which used the same cultivar for both the model development and validation in this experiment, demonstrated better overlap, further supporting our hypothesis on the possible presence of the cultivar effect. Despite this, the N THR strategy of Exp. 2 succeeded in reducing the N fertilizer inputs even under the assumption of the presence of cultivar effect and could be considered as a flexible model for optimizing N fertilization in different cultivars of processing tomato. However, developing a linear-plateau model adopted in N THR treatments is particularly time-consuming, as it requires the implementation of experimental design along different growing seasons and locations. Furthermore, the impact of more cropping conditions needs to be explored (e.g., soil type, residues of previous crop incorporated into the soil, and so forth). Nowadays, satellites are widespread in crop reflectance monitoring, and the reflectance of past growing seasons can be easily obtained. Ideally, farmers aided by agronomists and technicians could monitor the reflectance of their fields in the past years, which are assumed to be under non-limiting N conditions. The curve obtained for the GVI over the GDDs could be used as a location-specific model, and even a cultivar-specific one, as was done for N SPY_{EVO}. However, we are aware of the strong limitation of the N SPY_{EVO} model developed in our experiment (Fig. 1d), as it was built considering only one growing season. Indeed, the pattern of vegetation indices may change across different growing seasons. However, in our experiment, the GVI profile of N180 in Exp. 2 overlapped with the threshold model EVO (Fig. 4b), suggesting possible stability along multiple growing seasons. Using the GDDs as a timescale unit instead of the DAT could have enabled the temporal transferability of the GVI pattern, as already demonstrated by former authors (Li et al. 2022b). However, due to the limited data available, we recommend further analyzing this topic by monitoring the GVI profile along GDDs in different growing seasons in the same location. Alternative timescales, such as the cumulative potential evapotranspiration ET_0 (González-Gómez et al. 2018), could also be tested.

Tomato physiology was not affected by dynamic N fertilization (Table 5), although a lower N rate was supplied compared to N180. This is in contrast with the literature, where higher N supply is commonly associated with higher photosynthesis (Cechin and de Fátima Fumis 2004; Kull 2002) because of the key role of N in the photosynthetic enzyme Rubisco (Schulze et al. 1994). Also, reduced instantaneous transpiration and WUE_L were observed in crops under N deficiency (Zhou et al. 2020). This further confirms that dynamic N management strategies do not limit the crop performances, in agronomic terms, nor the physiological aspects, as tomatoes were maintained under optimal N status by matching the N supply with the crop N requirements.

Considering the yield composition, dynamic N strategies reduced the total and marketable fruit number per plant in Exp. 1 and Exp. 2 (Fig. 5a and 5b). Conversely, the average marketable fruit weight was increased in Exp. 1 (Fig. 5c). Coherently with our finding, an increase in fruit size in cantaloupe under dynamic N fertilization was observed in Gianquinto et al. (2010). Furthermore, dynamic N strategies increased the percentage of healthy and ripe fruits and reduced the incidence of sunburned and rotten fruits (Fig. 5d), as similarly observed by Ronga et al. (2020), possibly as a cause of lower nutritional disorders. Although no significant effect was observed in different quality parameters (EC, pH, dry matter content, and lycopene Supplementary material S5), dynamic N strategies improved the sugar accumulation in fruits (°Brix) in Exp. 2 (Fig. 6), as already reported for cantaloupe by Gianquinto et al. 2010. In tomatoes, moderate N fertilization can result in increased sugar

accumulation in fruits compared to high N fertilization (Ronga et al. 2020; Parisi et al. 2004) associated with a lower demand for carbon skeleton for amino acid and protein biosynthesis (Wingler et al. 2006), although the response of lycopene concentration to N fertilization could be cultivar-specific (Frías-Moreno et al. 2020). Therefore, reducing N inputs up to the minimum critical rate through dynamic N fertigation enabled us to maintain the same yield level without worsening the overall quality of the fruit and, in some cases, improving it (e.g., °Brix).

4.2. GHG emissions analysis

Nitrous oxide (N_2O) stands among the major GHG in the agricultural sector (Balafoutis et al. 2017). Originating from the microbial denitrification of the NO_3^- in soil (Balafoutis et al. 2017), N_2O is responsible for 58.6 % of the total emissions associated with N fertilizers (Menegat et al. 2022). In the cultivation stage of processing tomato, total GHG emissions per t of product were quantified by Ronga et al. (2019a) in 55.16 kg CO_2eq t^{-1}. In particular, the manufacturing of N fertilizers and field emissions of N_2O by N fertilizers represent 23 % of the GHG emissions (12.7 kg CO_2eq t^{-1}, Ronga et al. 2019a). In our analysis, the GHG emissions associated with the N_2O volatilization, atmospheric deposition (indirect emissions), and N fertilizers manufacturing in the fertilized control accounted for slightly lower values (9.5 kg CO_2eq t^{-1}). In our assessment, the emission of N_2O following the N application was calculated considering the specific equation developed for drip-irrigation systems (Kuang et al. 2021). Kuang et al. (2021) have clarified that drip irrigation systems determine a restricted amount of N_2O volatilization, resulting in a lower emission factor than the commonly adopted emission factor proposed by the IPCC guidelines. Furthermore, we did not account for the N leaching and N runoff in indirect emissions, as they are omitted from drip-irrigation systems (Hergoulac'h et al. 2019). Adopting dynamic N management strategies, the GHG emissions intensity associated with N fertilization can be significantly reduced by about 45 % (Fig. 7). Recently, Ruan et al. (2024) showed that precision N management could reduce the GHG intensity in winter wheat up to 38 % in China. This is of utmost importance considering that N fertilizers contribute to 11–13 % of total agricultural GHG emissions (Menegat et al. 2022; FAO 2020). However, we highlight that further assessments are needed to consider the GHG emissions associated with the reflectance sensor production, which were not voluntarily considered in our assessment.

5. Conclusions

The present study clearly shows how the dynamic fertilization of N guided by the GVI can help growers significantly reduce the amount of N fertilizers applied in processing tomatoes cultivation, avoiding yield losses, fostering the objective to reduce by 20% fertilizer use set by the European Farm to Fork Strategy, and drastically improving the agronomic, economic and environmental performances. Among the different strategies explored, those based on the absolute threshold values of GVI (e.g., N THR), overcome the logistical limitation associated with the use of a well-fertilized plot in the field (e.g., including the implementation of an independent irrigation system), and even improving the performances in terms of NUE and GHG emissions compared to the N SPY strategy. In this regard, developing specific linear-plateau models for cultivars, locations, or cultural conditions might require a significant effort dedicated to experimental setup replicated in different growing seasons, which could slow the development, and thus the adoption, of dynamic N fertilization strategies. The N SPY_{EVO} addresses such an issue using the GVI monitored in a well-fertilized spy plot from the previous year. This could be replicated by using satellites to monitor the location-specific reflectance in previous years. Despite the optimal performances and the inherent simplicity associated with the N SPY_{EVO} management, the stability of the GVI profile along the GDDs should be checked over multiple growing seasons. Seed companies test new cultivars in field trials under farming conditions, usually in different locations and growing seasons. Monitoring the optimal GVI curve of each cultivar can be an added value for the marketing strategies of breeders and seed companies that propose the new cultivar in the market, which might stimulate the adoption of dynamic fertigation by farmers. We must underline, however, that each dynamic threshold model was validated in only one-year field experiments: however, based on the first validation results shown in this paper, we recommend focusing efforts on further validation of the N SPY_{EVO} threshold model, as it has the potentiality to maintain similar agronomic performances with limited efforts in model development. Finally, integrating the N balance computation with dynamic N strategies was validated as a quick tool to calculate the optimal N rate to be supplied when the dynamic N management strategy recommends a fertigation. Based on the positive performances of the dynamic N management strategies that emerged from this study, scaling them to open-field farms with the adoption of airborne sensors (drones or satellites) deserves the attention of further research.

CRediT authorship contribution statement

Vito Aurelio Cerasola: Writing – original draft, Visualization, Methodology, Investigation, Formal analysis, Data curation, Conceptualization. **Stefano Bona:** Writing – review & editing, Validation, Formal analysis, Data curation. **Daniele Borsato:** Methodology, Investigation, Conceptualization. **Luca Gavioli:** Investigation. **Gaia Moretti:** Investigation. **Luigi Manfrini:** Investigation. **Giuseppina Pennisi:** Writing – review & editing, Visualization, Validation. **Francesco Orsini:** Writing – review & editing, Validation, Project administration, Funding acquisition. **Enrico Buscaroli:** Methodology, Investigation, Writing – review & editing. **Paolo Sambo:** Investigation, Conceptualization. **Giorgio Gianquinto:** Writing – review & editing, Supervision, Methodology, Conceptualization.

Declaration of competing interest

The authors declare that they have no known competing financial interests or personal relationships that could have appeared to influence the work reported in this paper.

Acknowledgements

This paper is (partially) supported by the PRIMA program under grant agreement No 2242, project FrontAg Nexus. The PRIMA program is supported by the European Union. Furthermore, the paper is (partially) supported by the European Union Next-GenerationEU (PIANO NAZIONALE DI RIPRESA E RESILIENZA (PNRR) – MISSIONE 4 COMPONENTE 2, INVESTIMENTO 1.4 – D.D. 1032 17/06/2022, CN00000022) within the Agritech National Research Center. This manuscript reflects only the authors' views and opinions, neither the European Union nor the European Commission can be considered responsible for them. Furthermore, we sincerely acknowledge Massimiliano Beretta from ISI Sementi for sharing the seeds materials used in the second experiment, and Agata Morelli for accuratethe English proofreading.

Supplementary materials

Supplementary material associated with this article can be found, in the online version, at doi:10.1016/j.scienta.2025.114124.

Data availability

Data will be made available on request.

References

Allen, R.G., Pereira, L.S., Raes, D., Smith, M., 1998. FAO Irrigation and Drainage Paper 56. Crop Evapotranspiration. Guidelines for Computing Crop Water Requirements. FAO, Rome.

Appolloni, E., Pennisi, G., Paucek, I., Cellini, A., Crepaldi, A., Spinelli, F., Gianquinto, G., Gabarrell, X., Orsini, F., 2023. Potential application of pre-harvest LED interlighting to improve tomato quality and storability. Postharvest. Biol. Technol. 195, 112113. https://doi.org/10.1016/j.postharvbio.2022.112113.

Balafoutis, A., Beck, B., Fountas, S., Vangeyte, J., Van der Wal, T., Soto, I., Gómez-Barbero, M., Barnes, A., Eory, V., 2017. Precision agriculture technologies positively contributing to GHG emissions mitigation, farm productivity and economics. Sustainability 9 (8), 1339. https://doi.org/10.3390/su9081339.

Baty, F., Ritz, C., Charles, S., Brutsche, M., Flandrois, J.P., Delignette-Muller, M.L., 2015. A toolbox for nonlinear regression in R: the package nlstools. J. Stat. Soft. 66, 1–21. https://doi.org/10.18637/jss.v066.i05.

Blackmer, T.M., Schepers, J.S., 1995. Use of a chlorophyll meter to monitor nitrogen status and schedule fertigation for corn. J. Prod. Agric. 8 (1), 56–60. https://doi.org/10.2134/jpa1995.0056.

Cechin, I., de Fátima Fumis, T., 2004. Effect of nitrogen supply on growth and photosynthesis of sunflower plants grown in the greenhouse. Plant Sci. 166 (5), 1379–1385. https://doi.org/10.1016/j.plantsci.2004.01.020.

Cerasola, V.A., Orsini, F., Pennisi, G., Moretti, G., Bona, S., Mirone, F., Verrelst, J., Berger, K., Gianquinto, G., 2025. Hyperspectral imaging for precision nitrogen management: a comparative exploration of two methodological approaches to estimate optimal nitrogen rate in processing tomato. Smart Agr. Technol., 100802 https://doi.org/10.1016/j.atech.2025.100802.

Cerasola, V.A., Pennisi, G., Orsini, F., Bona, S., Gianquinto, G., 2023. Hybridization of vegetation index with agroclimatic data to improve biomass estimation in tomato for precision N management. In: 2023 IEEE International Workshop on Metrology for Agriculture and Forestry (MetroAgriFor). IEEE, pp. 86–91.

Cerasola, V.A., Perlotti, L., Pennisi, G., Orsini, F., Gianquinto, G., 2022. Potential use of superabsorbent polymer on drought-stressed processing tomato (Solanum lycopersicum L.) in a Mediterranean climate. Horticulturae 8 (8), 718. https://doi.org/10.3390/horticulturae8080718.

Cilia, C., Panigada, C., Rossini, M., Meroni, M., Busetto, L., Amaducci, S., Boschetti, M., Picchi, V., Colombo, R., 2014. Nitrogen status assessment for variable rate fertilization in maize through hyperspectral imagery. Remote Sens. 6 (7), 6549–6565. https://doi.org/10.3390/rs6076549.

Crusiol, L.G.T., Carvalho, J.D.F.C., Sibaldelli, R.N.R., Neiverth, W., do Rio, A., Ferreira, L. C., Procópio, S.O., Mertz, L.M., Nemopuceno, A.L., Neumaier, N., Farias, J.R.B., 2017. NDVI variation according to the time of measurement, sampling size, positioning of sensor and water regime in different soybean cultivars. Precision Ag 18, 470–490. https://doi.org/10.1007/s11119-016-9465-6.

De Souza, R., Grasso, R., Peña-Fleitas, M.T., Gallardo, M., Thompson, R.B., Padilla, F.M., 2020. Effect of cultivar on chlorophyll meter and canopy reflectance measurements in cucumber. Sensors 20 (2), 509. https://doi.org/10.3390/s20020509.

Emilia-Romagna, 2022. Disciplinari Di Produzione Integrata\Norme Generali, Bologna. https://agricoltura.regione.emilia-romagna.it/produzioni-agroalimentari/agricoltura-sostenibile/agricoltura-integrata/Collezione-dpi/dpi_2022/norme-generali-2022 (accessed 18 February 2025).

European Commission, 2020. Farm to fork strategy: for a fair, healthy and environmentally-friendly food system. In: Communication from the Commission to the European Parliament, the Council, the European Economic and Social Committee and the Committee of the Regions, 381, pp. 1–9. https://eur-lex.europa.eu/legal-content/EN/TXT/?uri=CELEX:52020DC0381 (accessed 22/02/2025).

Erdal, I., Ertek, A., Şenyiğit, U., Yılmaz, H.İ., 2006. Effects of different irrigation programs and nitrogen levels on nitrogen concentration, uptake and utilisation in processing tomatoes (Lycopersicum esculentum). Aust. J. Exp. Agric. 46 (12), 1653–1660. https://doi.org/10.1071/EA04252.

FAO, 2020. Emissions due to agriculture. Global, regional and country trends 2000–2018. FAOSTAT Analytical Brief Series No 18. https://openknowledge.fao.org/items/08e67acd-1791-4486-ba41-2b52a075b432 (accessed 22/02/2025).

Fernandes, F.M., Soratto, R.P., Fernandes, A.M., Souza, E.F., 2021. Chlorophyll meter-based leaf nitrogen status to manage nitrogen in tropical potato production. Agron. J. 113 (2), 1733–1746. https://doi.org/10.1002/agj2.20589.

Fox, J., Weisberg, S., 2018. An R companion to Applied Regression, 3rd ed. Sage publications.

Frías-Moreno, M.N., Espino-Díaz, M., Dávila-Aviña, J., Gonzalez-Aguilar, G.A., Ayala-Zavala, J.F., Molina-Corral, F.J., Parra-Quezada, R.A., Orozco, G.I.O., 2020. Preharvest nitrogen application affects quality and antioxidant status of two tomato cultivars. Bragantia 79, 134–144. https://doi.org/10.1590/1678-4499.20190247.

Gianquinto, G., Fecondini, M., Mezzetti, M., Orsini, F., 2010. Steering nitrogen fertilisation by means of portable chlorophyll meter reduces nitrogen input and improves quality of fertigated cantaloupe (Cucumis melo L. var. cantalupensis Naud.). J. Sci. Food Agric. 90 (3), 482–493. https://doi.org/10.1002/jsfa.3843.

Gianquinto, G., Orsini, F., Fecondini, M., Mezzetti, M., Sambo, P., Bona, S., 2011a. A methodological approach for defining spectral indices for assessing tomato nitrogen status and yield. Eur. J. Agron. 35 (3), 135–143. https://doi.org/10.1016/j.eja.2011.05.005.

Gianquinto, G., Orsini, F., Pennisi, G., Bona, S., 2019. Sources of variation in assessing canopy reflectance of processing tomato by means of multispectral radiometry. Sensors 19 (21), 4730. https://doi.org/10.3390/s19214730.

Gianquinto, G., Orsini, F., Sambo, P., D'Urzo, M.P., 2011b. The use of diagnostic optical tools to assess nitrogen status and to guide fertilization of vegetables. HortTechnology 21 (3), 287–292. https://doi.org/10.21273/HORTTECH.21.3.287.

Gianquinto, G., Sambo, P., Borsato, D., 2004. Determination of SPAD threshold values for the optimisation of nitrogen supply in processing tomato. Acta Hortic. https://doi.org/10.17660/ActaHortic.2006.700.26.

Gianquinto, G., Sambo, P., Pimpini, F., 2001. The use of SPAD-502 chlorophyll meter for dynamically optimizing the nitrogen supply in potato crop: first results. Acta Hortic. https://doi.org/10.17660/ActaHortic.2003.627.29.

González-Gómez, L., Campos, I., Calera, A., 2018. Use of different temporal scales to monitor phenology and its relationship with temporal evolution of normalized difference vegetation index in wheat. J. Appl. Remote Sens. 12 (2). https://doi.org/10.1117/1.JRS.12.026010, 026010-026010.

Hargreaves, G.H., Samani, Z.A., 1985. Reference crop evapotranspiration from temperature. Appl. Eng. Agric. 1 (2), 96–99.

Hartz, T.K., Bottoms, T.G., 2009. Nitrogen requirements of drip-irrigated processing tomatoes. HortScience 44 (7), 1988–1993. https://doi.org/10.21273/HORTSCI.44.7.1988.

Hebebrand, C., Laborde Debucquet, D., 2023. High fertilizer prices contribute to rising global food security concerns. In: Glauber, Joseph, Laborde Debucquet, David (Eds.), The Russia-Ukraine Conflict and Global Food Security. https://doi.org/10.2499/9780896294394_07. Section One: A Conflict with Global Consequences.

Hergoualc'h, K., Akiyama, H., Bernoux, M., Chirinda, N., Prado, A.D., Kasimir, Å., MacDonald, J.D., Ogle, S.M., Regina, K., Weerden, T.J.V.D., 2019. N2O emissions from managed soils, and CO2 emissions from lime and urea application. Refinement to the 2006 IPCC Guidelines for National Greenhouse Gas Inventories, Chapter 11. Intergovernmental Panel on Climate Change (IPCC) (2019).

HESQ, Y., Fossum, J.P., 2014. Calculation of carbon footprint of fertilizer production. Des. Pilot Plant Recover. Ammon. Salts WWTP Residual Water 76.

Houles, V., Guerif, M., Mary, B., 2007. Elaboration of a nitrogen nutrition indicator for winter wheat based on leaf area index and chlorophyll content for making nitrogen recommendations. Eur. J. Agron. 27 (1), 1–11. https://doi.org/10.1016/j.eja.2006.10.001.

Incrocci, L., Thompson, R.B., Fernandez-Fernandez, M.D., De Pascale, S., Pardossi, A., Stanghellini, C., Rouphael, Y., Gallardo, M., 2020. Irrigation management of European greenhouse vegetable crops. Agric. Water Manag. 242, 106393. https://doi.org/10.1016/j.agwat.2020.106393.

Kuang, W., Gao, X., Tenuta, M., Zeng, F., 2021. A global meta-analysis of nitrous oxide emission from drip-irrigated cropping system. Glob. Change Biol. 27 (14), 3244–3256. https://doi.org/10.1111/gcb.15636.

Kull, O., 2002. Acclimation of photosynthesis in canopies: models and limitations. Oecologia 133, 267–279. https://doi.org/10.1007/s00442-002-1042-1.

Lenth, R., 2022. emmeans: estimated marginal means, aka least-squares means. R package version 1.7. 2.

Li, X., Ata-UI-Karim, S.T., Li, Y., Yuan, F., Miao, Y., Yoichiro, K., Cheng, T., Tang, L., Tian, X., Liu, X., Tian, Y., Zhu, Y., Cao, W., Cao, Q., 2022a. Advances in the estimations and applications of critical nitrogen dilution curve and nitrogen nutrition index of major cereal crops. A review. Comput. Electron. Agric. 197, 106998. https://doi.org/10.1016/j.compag.2022.106998.

Li, Z., Zhao, Y., Taylor, J., Gaulton, R., Jin, X., Song, X., Li, Z., Meng, Y., Chen, P., Feng, H., Wang, C., Guo, W., Xu, X., Chen, L., Yang, G., 2022b. Comparison and transferability of thermal, temporal and phenological-based in-season predictions of above-ground biomass in wheat crops from proximal crop reflectance data. Remote Sens. Environ. 273, 112967. https://doi.org/10.1016/j.rse.2022.112967.

Mariotti, M., Andreuccetti, V., Arduini, I., Minieri, S., Pampana, S., 2018. Field bean for forage and grain in short-season rainfed Mediterranean conditions. Ital. J. Agron. 13 (3), 208–215. https://doi.org/10.4081/ija.2018.1112.

Menegat, S., Ledo, A., Tirado, R., 2022. Greenhouse gas emissions from global production and use of nitrogen synthetic fertilisers in agriculture. Sci. Rep. 12 (1), 1–13. https://doi.org/10.1038/s41598-022-18773-w.

Medrano, H., Tomás, M., Martorell, S., Flexas, J., Hernández, E., Rosselló, J., Pou, A., Esclona, J.M., Bota, J., 2015. From leaf to whole-plant water use efficiency (WUE) in complex canopies: limitations of leaf WUE as a selection target. Crop J. 3 (3), 220–228. https://doi.org/10.1016/j.cj.2015.04.002.

Miguez, F., 2022. Nonlinear regression for agricultural applications [R package nlraa version 1.5]. https://CRAN.R-project.org/package=nlraa.

Moreno-García, B., Casterad, M.A., Guillén, M., Quílez, D., 2018. Agronomic and economic potential of vegetation indices for rice N recommendations under organic and mineral fertilization in Mediterranean regions. Remote Sens. 10 (12), 1908. https://doi.org/10.3390/rs10121908.

Oliveira, T.F., Pinto, F.A., Silva, D.J., 2019. Spectral vegetation indexes applied to nitrogen sufficiency index: a strategy with potential to increase nitrogen use efficiency on tomato crop. Eng. Agríc. 39, 118–126. https://doi.org/10.1590/1809-4430-Eng.Agric.v39n1p118-126/2019.

Padilla, F.M., Farneselli, M., Gianquinto, G., Tei, F., Thompson, R.B., 2020. Monitoring nitrogen status of vegetable crops and soils for optimal nitrogen management. Agric. Water Manag. 241. https://doi.org/10.1016/j.agwat.2020.106356, 106356.

Padilla, F.M., Karaca, C., Peña-Fleitas, M.T., Gallardo, M., Rodríguez, A., Thompson, R. B., 2024. Cultivar effect on proximal optical sensor measurements and estimation of leaf N content in muskmelon and sweet pepper. Eur. J. Agron. 159, 127249. https://doi.org/10.1016/j.eja.2024.127249.

Padilla, F.M., Peña-Fleitas, M.T., Gallardo, M., Thompson, R.B., 2017. Determination of sufficiency values of canopy reflectance vegetation indices for maximum growth and yield of cucumber. Eur. J. Agron. 84, 1–15. https://doi.org/10.1016/j.eja.2016.12.007.

Padilla, F.M., Peña-Fleitas, M.T., Gallardo, M., Thompson, R.B., 2015. Threshold values of canopy reflectance indices and chlorophyll meter readings for optimal nitrogen nutrition of tomato. Ann. Appl. Biol. 166 (2), 271–285. https://doi.org/10.1111/aab.12181.

Parisi, M., Giordano, L., Pentangelo, A., D'onofrio, B., Villari, G., 2004. Effects of different levels of nitrogen fertilization on yield and fruit quality in processing tomato. Acta Hortic. https://doi.org/10.17660/ActaHortic.2006.700.19.

Peñuelas, J., Coello, F., Sardans, J., 2023. A better use of fertilizers is needed for global food security and environmental sustainability. Agr. Food Secur. 12 (1), 1–9. https://doi.org/10.1186/s40066-023-00409-5.

Petropoulos, S.A., Fernandes, Â., Xyrafis, E., Polyzos, N., Antoniadis, V., Barros, L., CFR Ferreira, I., 2020. The optimization of nitrogen fertilization regulates crop performance and quality of processing tomato (Solanum lycopersicum L. cv. Heinz 3402). Agronomy 10 (5), 715. https://doi.org/10.3390/agronomy10050715.

Pinter Jr, P.J., Jackson, R.D., Elaine Ezra, C., Gausman, H.W., 1985. Sun-angle and canopy-architecture effects on the spectral reflectance of six wheat cultivars. Int. J. Remote Sens. 6 (12), 1813–1825. https://doi.org/10.1080/01431168508948330.

Rajarathinam, A., Vetriselvi, R., 2017. Modeling cereals crop production based on parametric and non-parametric models. Int. J. Agric. Stat. Sci. Vol, 13 (1), 17–28.

Ravier, C., Jeuffroy, M.H., Meynard, J.M., 2016. Mismatch between a science-based decision tool and its use: the case of the balance-sheet method for nitrogen fertilization in France. NJAS-Wageningen J. Life Sci. 79, 31–40. https://doi.org/10.1016/j.njas.2016.10.001.

Rodríguez, A., Peña-Fleitas, M.T., Gallardo, M., de Souza, R., Padilla, F.M., Thompson, R. B., 2020. Sweet pepper and nitrogen supply in greenhouse production: critical nitrogen curve, agronomic responses and risk of nitrogen loss. Eur. J. Agron. 117, 126046. https://doi.org/10.1016/j.eja.2020.126046.

Ronga, D., Gallingani, T., Zaccardelli, M., Perrone, D., Francia, E., Milc, J., Pecchioni, N., 2019a. Carbon footprint and energetic analysis of tomato production in the organic vs the conventional cropping systems in Southern Italy. J. Clean. Prod. 220, 836–845. https://doi.org/10.1016/j.jclepro.2019.02.111.

Ronga, D., Parisi, M., Pentangelo, A., Mori, M., Di Mola, I., 2019b. Effects of nitrogen management on biomass production and dry matter distribution of processing tomato cropped in southern Italy. Agronomy 9 (12), 855. https://doi.org/10.3390/agronomy9120855.

Ronga, D., Pentangelo, A., Parisi, M., 2020. Optimizing N fertilization to improve yield, technological and nutritional quality of tomato grown in high fertility soil conditions. Plants 9 (5), 575. https://doi.org/10.3390/plants9050575.

Ruan, G., Cammarano, D., Ata-UI-Karim, S.T., Liu, X., Tian, Y., Zhu, Y., Cao, W., Cao, Q., 2024. Investigating data-driven approaches to optimize nitrogen recommendations for winter wheat. Comput. Electron. Agric. 220, 108857. https://doi.org/10.1016/j.compag.2024.108857.

Samborski, S.M., Tremblay, N., Fallon, E., 2009. Strategies to make use of plant sensors-based diagnostic information for nitrogen recommendations. Agron. J. 101 (4), 800–816. https://doi.org/10.2134/agronj2008.0162Rx.

Schulze, E.D., Kelliher, F.M., Korner, C., Lloyd, J., Leuning, R., 1994. Relationships among maximum stomatal conductance, ecosystem surface conductance, carbon assimilation rate, and plant nitrogen nutrition: a global ecology scaling exercise. Annu. Rev. Ecol. Syst. 629–660.

Tei, F., Benincasa, P., Guiducci, M., 2002. Critical nitrogen concentration in processing tomato. Eur. J. Agron. 18 (1–2), 45–55. https://doi.org/10.1016/S1161-0301(02)00096-5.

Tei, F., Benincasa, P., Farneselli, M., Tosti, G., Guiducci, M., 2015. Environmentally sustainable nitrogen nutrition management in processing tomato. Acta Hortic. 41–48, 1081.

Tei, F., De Neve, S., de Haan, J., Kristensen, H.L., 2020. Nitrogen management of vegetable crops. Agric. Water Manage. 240, 106316. https://doi.org/10.1016/j.agwat.2020.106316.

Vadillo, J.M., Gimenez, M.C., Campillo, C., González, V., Prieto, M.H., 2022. Development of a methodology to characterize the nitrogen nutritional status of open field processing tomato by means of fast indicators. Acta Hortic. https://doi.org/10.17660/ActaHortic.2022.1351.14.

Valenzuela, H., 2024. Optimizing the nitrogen use efficiency in vegetable crops. Nitrogen 5 (1), 106–143. https://doi.org/10.3390/nitrogen5010008.

Vos, J., Struik, P.C., 1992. Crop responses to nitrogen. In: Meulenbroek, J.L. (Ed.), Proc. Congr. Agriculture and environment in Eastern Europe and The Netherlands, pp. 195–205. Wageningen, The Netherlands.

Wingler, A., Purdy, S., MacLean, J.A., Pourtau, N., 2006. The role of sugars in integrating environmental signals during the regulation of leaf senescence. J. Exp. Bot. 57 (2), 391–399. https://doi.org/10.1093/jxb/eri279.

World Bank, 2024. https://blogs.worldbank.org/en/opendata/fertilizer-prices-edge-lower-amid-lower-input-costs-and-improved (accessed 15 July 2024).

Zeka, E., Skreli, E., 2022. The impact of the Russia-Ukraine conflict on the profitability of agricultural farms. BRIDGE'22 09_10 DEC, 198.

Zheng, H.L., Liu, Y.C., Qin, Y.L., Yang, C.H.E.N., Fan, M.S., 2015. Establishing dynamic thresholds for potato nitrogen status diagnosis with the SPAD chlorophyll meter. J. Integr. Agric. 14 (1), 190–195. https://doi.org/10.1016/S2095-3119(14)60925-4.

Zhou, H., Kang, S., Li, F., Du, T., Shukla, M.K., Li, X., 2020. Nitrogen application modified the effect of deficit irrigation on tomato transpiration, and water use efficiency in different growth stages. Sci. Hortic. 263, 109112. https://doi.org/10.1016/j.scienta.2019.109112.

Ziadi, N., Bélanger, G., Gastal, F., Claessens, A., Lemaire, G., Tremblay, N., 2009. Leaf nitrogen concentration as an indicator of corn nitrogen status. Agron. J. 101 (4), 947–957. https://doi.org/10.2134/agronj2008.0172x.